

# Successive, Seed-Mediated Growth for the Synthesis of Single-Crystal Gold Nanospheres with Uniform Diameters Controlled in the Range of 5–150 nm

Yiqun Zheng, Xiaolan Zhong, Zhiyuan Li, and Younan Xia\*

A simple and robust route is described to the synthesis of single-crystal Au nanospheres with diameters controlled in the range of 5 nm to 150 nm. The success of this synthesis relies on the use of single-crystal Au spheres with different diameters as the seeds for successive growth and the use of a slow injection rate for the precursor to enable surface diffusion for the atoms added onto the surface of a seed. The diameters could be precisely controlled by varying the size and/or number of the seeds. The products exhibit excellent uniformity in terms of both size and shape and they are expected to find widespread use in a number of applications, including self-assembly, fabrication of metallo dielectric photonic crystals, plasmonics, and biomedical research.

## 1. Introduction

Gold (Au) nanocrystals have attracted enormous research interests owing to their remarkable physicochemical properties and potential applications in the optical and catalytic fields.<sup>[1–11]</sup> It is well accepted that the physicochemical properties of Au nanocrystals are highly dependent on their sizes and shapes.<sup>[12–16]</sup> For instance, as the particle increases in size, the localized surface plasmon resonance (LSPR) peak clearly exhibits a red-shift, as confirmed by both theoretical calculations and experimental observations.<sup>[17,18]</sup> It has also been reported that the sharp edges and corners or high-index facets on the surface of Au nanocrystals can positively impact their catalytic performance.<sup>[19–21]</sup> To this end, it has become highly desirable to develop synthetic protocols for generating Au nanocrystals with a precise control over both size and shape. Thanks to

research efforts from many groups, it is now possible to produce Au nanocrystals enclosed with different proportions of the three low-index facets: {100}, {111}, and {110}. Notable examples can be found in both single-crystal structures (cubes, octahedrons, cuboctahedrons, tetrahedrons, rhombic dodecahedrons, and rods)<sup>[22–27]</sup> and twinned structures (decahedra, icosahedra, wires, and prisms).<sup>[28–31]</sup> Recent progress has also enabled the synthesis of Au nanocrystals encased by high-index facets, such as trisoctahedrons with {221} facets, tetrahexahedrons with {037} facets, truncated ditetragonal prisms with {310} facets, concave cubes with {720} facets, and hexoctahedrons with {321} facets.<sup>[31–35]</sup>

Despite these successful demonstrations, we noticed that the synthesis of Au nanocrystals with a truly spherical shape and precisely controlled sizes has been met with limited success. Compared with the nonspherical counterparts, it is much easier to work with a spherical particle in fundamental studies such as a computational simulation.<sup>[36]</sup> The spherical particles can serve as building blocks for self-assembly and construction of metallo dielectric photonic crystals.<sup>[37]</sup> They can also serve as probes, markers, or carriers for a variety of biomedical studies, including those related to the cellular uptake of nanoparticles, biodistribution and targeting efficacy of nanoparticles, and drug delivery.<sup>[38–42]</sup> In addition, the use of spherical particles with a single-crystal structure as the seeds could provide a simple model system to study seed-mediated growth. Given that the proportions of {111} and {100} facets on their surfaces are roughly the same, it would be convenient to monitor the shape evolution and thus single out the factors that determine the shape displayed by a product. To this end, both Au and Ag spherical nanocrystals have been employed as the seeds to study the mechanism(s) responsible for shape evolution during seed-mediated growth.<sup>[43–47]</sup> As a result, synthesis of Au nanocrystals with a truly spherical shape and narrow size distributions should be beneficial to a variety of studies and applications.

Although a number of protocols have been reported for the synthesis of Au nanospheres, the products were mainly polycrystalline structures marked by a quasi-spherical shape.<sup>[48–60]</sup> In many cases, it is not so difficult to find sharp features on the particle surface and additional purification steps (for removal of non-spherical particles such as rods and plates) are often necessary to improve the percentage of quasi-spherical particles in

Y. Zheng, Prof. Y. Xia  
 School of Chemistry and Biochemistry  
 Georgia Institute of Technology  
 Atlanta, GA 30332, USA

E-mail: younan.xia@bme.gatech.edu  
 Dr. X. Zhong, Prof. Z. Y. Li  
 Institute of Physics

Chinese Academy of Sciences  
 Beijing 100080, P. R. China

Prof. Y. Xia  
 The Wallace H. Coulter Department of Biomedical Engineering  
 School of Chemical and Biomolecular Engineering  
 Georgia Institute of Technology  
 Atlanta, GA 30332, USA

DOI: 10.1002/ppsc.201300256



the final product.<sup>[48]</sup> The most successful attempt for the preparation of single-crystal Au nanocrystals with a spherical shape was based on overgrowth of single-crystal Au nanorods.<sup>[25]</sup> However, the use of Au nanorods longer than 20 nm makes it impossible to generate nanospheres with diameters smaller than 20 nm. The largest Au spheres that have been obtained from nanorod-based seeds were 41.3 nm in diameter. Recently, our group reported seed-mediated syntheses of single-crystal Au nanospheres with controlled diameters in the range of 5–30 nm.<sup>[44]</sup> Despite the high yield of single-crystal spheres, the largest size we could achieve was limited to 30 nm. Further attempt to increase the size resulted in non-spherical shapes. As a result, it remains a grand challenge to achieve a precise size control over a broad range up to 100 nm for single-crystal Au nanospheres.

Here, we present a facile and robust route to the synthesis of single-crystal Au nanospheres with their diameters increasingly tuned from 5 to 150 nm. The value of this work can be understood from the following aspects. First, for the first time, single-crystal Au nanocrystals with a spherical shape could be obtained with a diameter as large as 150 nm. Compared with the polycrystalline, quasi-spherical particles reported in previous publications, the current products not only had a single-crystal structure and truly spherical shape, but also exhibited excellent uniformity in terms of both size and shape. Second, the size of these single-crystal Au nanospheres could be precisely controlled in the range of 5–150 nm by varying the size or volume of the seeds. Finally, surface diffusion was identified as a critical parameter in determining the evolution of seeds into particles of increasing sizes without losing the spherical shape. In particular, a slow deposition rate for the atoms, enabled by dropwise addition of Au precursor and the presence of reductant at a low concentration, gives atoms added onto a seed enough time to diffuse across the surface, leading to the formation of a shape favored by thermodynamics.<sup>[61]</sup> In addition, the type of halide ions ( $\text{Br}^-$  and  $\text{I}^-$ ) present in the system was also investigated to reveal its role in the formation of Au nanocrystals with a truly spherical shape. We believe these nanospheres could find immediate use in the fabrication of multi-metallic nanostructures and metalloelectric photonic crystals.

## 2. Experimental Section

### 2.1. Chemicals and Materials

Gold(III) chloride trihydrate ( $\text{HAuCl}_4 \cdot 3\text{H}_2\text{O}$ , ≥99.9%), ascorbic acid (AA, ≥99.0%), sodium borohydride ( $\text{NaBH}_4$ , 98%), cetyltrimethylammonium bromide (CTAB, ≥99%), and cetyltrimethylammonium chloride (CTAC, 25 wt% in water) were all obtained from Sigma-Aldrich and used as received. In all experiments, we used deionized water with a resistivity of 18.2 M $\Omega$  cm, which was prepared using an ultrapure water system (Millipore, Billerica, MA). Aqueous  $\text{NaBH}_4$  solution ( $10 \times 10^{-3}$  M) was prepared by dissolving 15.1 mg of  $\text{NaBH}_4$  powder in 40 mL of water. The 10 mL syringe (part No. 309604) and syringe pump (part No. 14831200) were obtained from BD and Thermo Fisher Scientific, respectively.

### 2.2. Preparation of the Initial, CTAB-Capped Au Clusters

A fresh aqueous  $\text{NaBH}_4$  solution ( $10 \times 10^{-3}$  M, 0.6 mL) was rapidly added into a thoroughly mixed 10-mL aqueous solution containing  $\text{HAuCl}_4$  ( $0.25 \times 10^{-3}$  M) and CTAB ( $100 \times 10^{-3}$  M) using a pipette. A brown solution immediately formed upon the introduction of  $\text{NaBH}_4$ . The mixture was placed on an orbital shaker at a speed of 300 rpm for 2 min, and then kept undisturbed at 27 °C for 3 h to ensure complete decomposition of  $\text{NaBH}_4$  remaining in the reaction mixture.

### 2.3. Standard Procedure for the Preparation of Au Nanospheres with Diameters in the Range of 5–16 nm

Aqueous solutions of CTAC ( $200 \times 10^{-3}$  M, 2 mL), AA ( $100 \times 10^{-3}$  M, 1.5 mL), and the initial, CTAB-capped Au clusters were mixed in a 20-mL glass vial, followed by one-shot injection of an aqueous  $\text{HAuCl}_4$  solution ( $0.5 \times 10^{-3}$  M, 2 mL). See Table 1 for the volume of cluster solution and the corresponding diameter. The reaction was allowed to continue at 27 °C for 15 min. The product was collected by centrifugation at 14 500 rpm for 30 min, and then washed with water once for further use and characterization. The 10-nm Au nanospheres were dispersed in 1 mL of aqueous CTAC solution ( $20 \times 10^{-3}$  M) after washing, which was used as seeds in the second round of growth.

### 2.4. Standard Procedure for the Preparation of Au Nanospheres with Diameters in the Range of 15–80 nm

Aqueous solutions of CTAC ( $100 \times 10^{-3}$  M, 2 mL), AA ( $10 \times 10^{-3}$  M, 130  $\mu\text{L}$ ), and the 10-nm seeds were mixed in a 20-mL glass vial, followed by dropwise addition of aqueous  $\text{HAuCl}_4$  solution ( $0.5 \times 10^{-3}$  M, 2 mL) using a syringe pump at

**Table 1.** The average diameter ( $d_{av}$ ) and its standard deviation ( $\sigma$ ), the average hydrodynamic diameter ( $d_{hydro}$ ) and its standard deviation ( $\sigma_{hydro}$ ), the type of seed, and the volume (V) of seed solution for the Au nanospheres displayed in Figures 2, 3, and 4. The average diameter ( $d_{av}$ ) and its standard deviation were calculated from the TEM images by counting 50–100 particles. The average hydrodynamic diameter ( $d_{hydro}$ ) and its standard deviation were obtained from DLS measurements.

$d_{av}$ [nm]	$\sigma$ [%]	$d_{hydro}$ [nm]	$\sigma_{hydro}$ [%]	Type of seed	V [ $\mu\text{L}$ ]
5.2	0.52	n/a	n/a	Cluster	1000
8.0	0.54	n/a	n/a		500
10	0.81	n/a	n/a		50
16	1.6	26.81	35.6		20
15	1.1	26.25	42.2	10-nm sphere	300
23	1.1	36.46	34.8		100
46	1.9	58.55	20.2		10
80	1.3	103.0	26.8		5
70	1.5	103.5	14.1	46-nm sphere	1500
$1.0 \times 10^2$	3.1	131.9	23.2		500
$1.5 \times 10^2$	4.8	198.0	29.2		50

an injection rate of 2 mL h<sup>-1</sup>. See Table 1 for the volume of the 10-nm seed solution and the corresponding diameter. The reaction was allowed to proceed at 27 °C for 10 min after the injection had been finished. The final product was collected by centrifugation at 14 500 rpm for 10 min and washed with water once for characterization. The aqueous suspension of 46-nm Au nanospheres was mixed with 0.86 mL of water and then used as seeds for the third round of growth.

## 2.5. Standard Procedure for the Preparation of Au Nanospheres with Diameters in the Range of 70–150 nm

Aqueous solutions of CTAC ( $100 \times 10^{-3}$  M, 2 mL), AA ( $10 \times 10^{-3}$  M, 130 µL), and the 46-nm seed solution were mixed in a 20-mL glass vial, followed by dropwise addition of aqueous HAuCl<sub>4</sub> solution ( $0.5 \times 10^{-3}$  M, 2 mL) using a syringe pump. The injection rate was 2 mL h<sup>-1</sup>. See Table 1 for the volume of the 46-nm seed solution and the corresponding diameter. The reaction was allowed to proceed at 27 °C for 10 min after the injection had been finished. The final product was collected by centrifugation at 14 500 rpm for 10 min, and then washed with water once for characterization.

## 2.6. Instrumentation

Transmission electron microscopy (TEM) images were captured using a HT7700 microscope operated at 120 kV (Hitachi, Tokyo, Japan). The samples were prepared by dropping aqueous suspensions of the nanoparticles onto carbon-coated copper grids (part No. FCF200-Cu, Electron Microscopy Science, Hatfield, PA) and dried under ambient conditions in air. The dynamic light scattering (DLS) measurements were performed using Zetasizer Nano ZS (Malvern, Westborough, MA).

## 3. Results and Discussion

### 3.1. Size Control of Single-Crystal Au Nanospheres

**Figure 1** shows a schematic illustration of the procedure used for the preparation of Au nanospheres with diameters controlled in the range of 5–150 nm. In a typical process, HAuCl<sub>4</sub>, CTAC, and AA served as Au precursor, stabilizing agent, and reductant, respectively. More specifically, Au nanospheres with diameters in the range of 5–16 nm were obtained first by using CTAB-capped Au clusters as the seeds. In the following two steps, the 10- and 46-nm Au nanospheres were employed as the seeds to generate Au nanospheres with diameters in the range of 15–80 nm and 70–150 nm, respectively. It should be noted that the Au

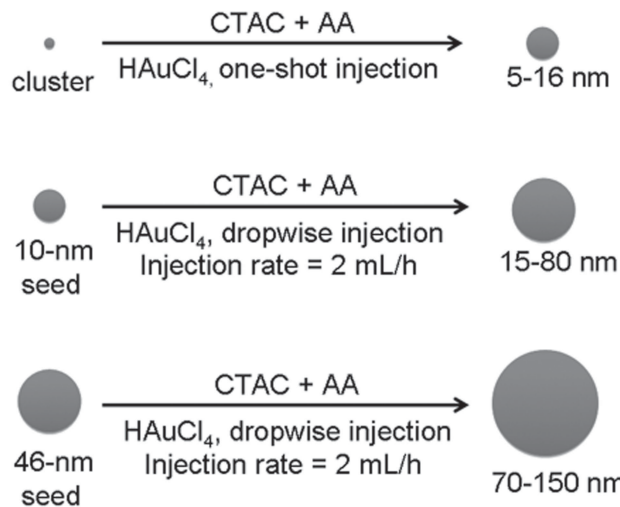


**Figure 1.** Schematics illustrating the successive growth procedure used for the preparation of Au nanospheres with controlled diameters increasingly tuned from 5 to 150 nm.

precursor solution had to be added into the reaction solution in one-shot injection with a pipette in the first step, whereas the Au precursor had to be added dropwise using a syringe pump in the second and third rounds of growth (see Section 3.2 for detailed discussion). **Figure 2** shows TEM images of Au nanospheres with diameters in the range of 5–16 nm that were prepared by seeding the growth with the initial, CTAB-capped

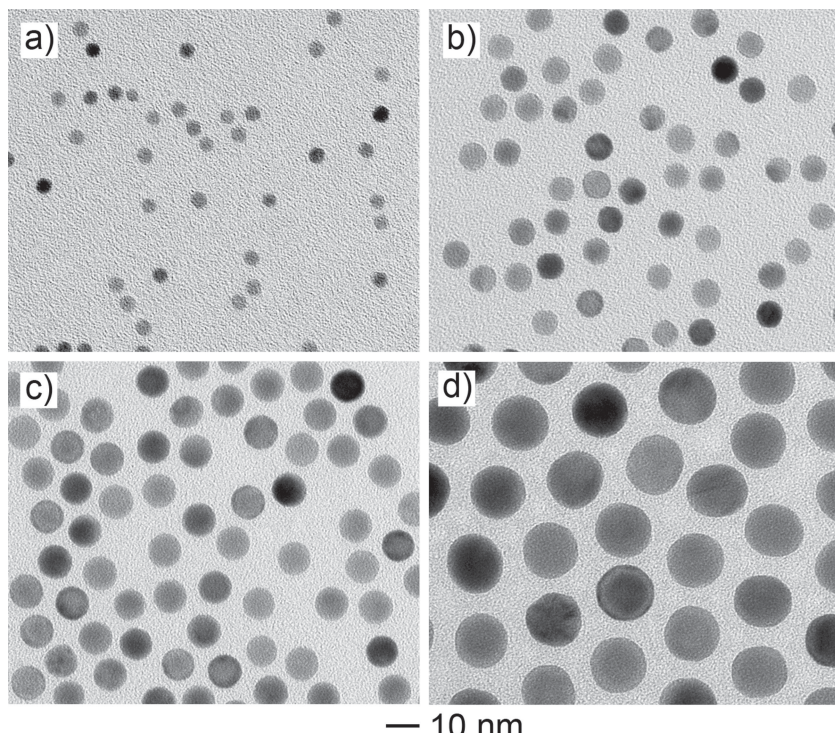


**Figure 2.** TEM images of single-crystal Au nanospheres with controlled diameters in the range of 5–16 nm: a) 5 nm; b) 8 nm; c) 10 nm; and d) 16 nm. They were obtained using the standard one-shot injection procedure, except that the volumes of the initial, CTAB-capped cluster solution were: a) 1000 µL; b) 500 µL; c) 50 µL; and d) 20 µL, respectively.

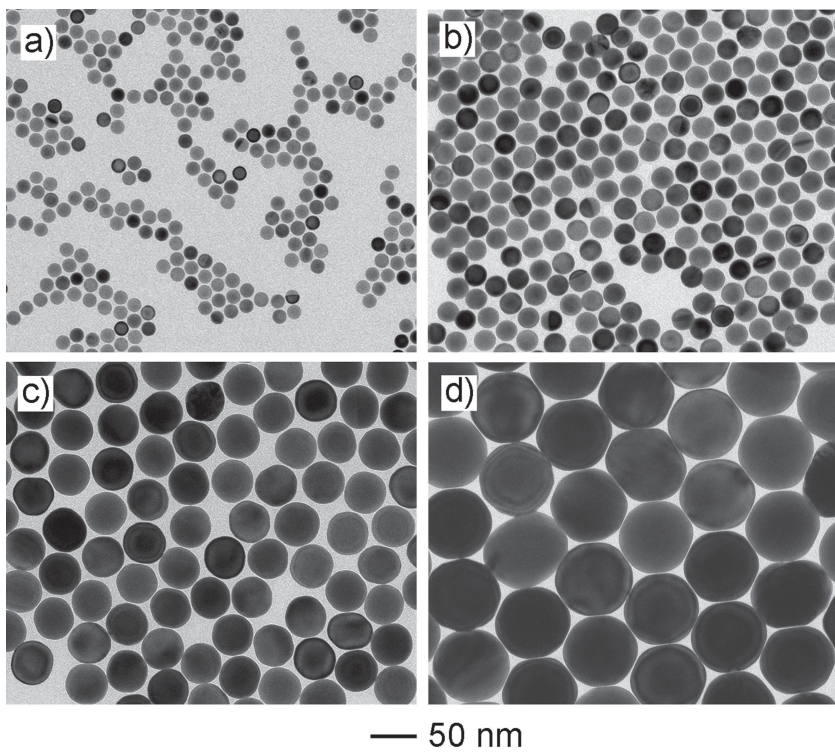


**Figure 3.** TEM images of single-crystal Au nanospheres with controlled diameters in the range of 15–80 nm: a) 15 nm; b) 23 nm; c) 46 nm; and d) 80 nm. They were obtained using the standard dropwise injection procedure, except that the volumes of the 10-nm seed solution were: a) 300  $\mu$ L; b) 100  $\mu$ L; c) 10  $\mu$ L; and d) 5  $\mu$ L, respectively.

Au clusters. The diameters of the Au nanospheres could be easily varied by controlling the volume of the cluster solution added into the reaction mixture. Specifically, when the volumes of the cluster solution were 1000, 500, 50, and 20  $\mu$ L, respectively, the diameters of the resultant nanospheres were 5, 8, 10, and 16 nm, respectively.

In the second round of growth, the as-prepared 10-nm Au nanospheres served as the seeds to generate Au nanospheres with diameters increasingly tuned from 15 to 80 nm. As shown in **Figure 3**, when the volumes of the 10-nm seed solution were 300, 100, 10, and 5  $\mu$ L, respectively, the diameters of the resultant nanospheres were tuned to 15, 23, 46, and 80 nm, respectively. The third round of growth used the same synthetic procedure as that for the second round except for the use of the as-prepared 46-nm Au nanospheres as the seeds. As shown in **Figure 4**, when the volumes of the 46-nm seed solution were 1500, 500, and 50  $\mu$ L, respectively, the resultant nanospheres were 70, 100, and 150 nm, respectively, in diameter. Beyond this size, the products tended to evolve into nonspherical particles (**Figure S1**, Supporting Information). The average diameter ( $d_{av}$ ), standard deviation ( $\sigma$ ), and percentage of spherical particles ( $f_s$ ), and detailed experimental conditions are summarized in Table 1. It should be noted that for each type of Au nanospheres, the standard deviation was less than 5% and the percentage of spherical particle was higher than 90%, indicating a high uniformity and purity for all the products.

To further validate the uniformity of our Au nanospheres, we also analyzed them using techniques other than electron

microscopy, including UV-vis extinction spectroscopy and DLS, that work with an ensemble of particles. **Figure S2** (Supporting Information) shows experimental and calculated UV-vis extinction spectra of Au nanospheres with different diameters. Both types of spectra displayed similar features in terms of extinction peak shape and position. Given the fact that the calculation was based on individual particles and the particle had a perfectly spherical shape, the matching of experimental and calculated spectra suggest that our Au nanospheres had a spherical shape as shown in the TEM images.

**Figure S3** (Supporting Information) shows DLS data from these Au nanospheres. Only one peak was observed for the size distribution of each sample of Au nanospheres, indicating its monodispersity in size. The average hydrodynamic diameters and standard deviations obtained from the DLS data are listed in Table 1. We noticed that the average hydrodynamic diameters were larger than the average diameters derived from the TEM images. Such differences could be attributed to the surfactant/solvation layer on the particle surface, such as water and CTAC molecules. In addition, the standard deviations obtained from DLS measurements differed significantly from those determined by TEM imaging. This discrepancy can be ascribed to

the procedure used for the transformation of the Fredholm first kind of equation in the DLS method, which is irrelevant to the characteristics of a colloidal suspension.<sup>[61]</sup> Similar widening of the size distribution in the DLS method has already been noted repeatedly in the literature.<sup>[62–64]</sup> Due to the presence of CTA micelles in the system, the DLS data of Au nanospheres of 5, 8, and 10 nm in diameter became unreliable so we decided not to include them. Taken together, we have characterized and confirmed the monodispersity of our Au nanospheres using TEM, UV-vis extinction spectra, and DLS.

### 3.2. The Effect of Injection rate for the Au Precursor

Unlike the one-shot injection of Au precursor in the first round, we had to add the Au precursor dropwise using a syringe pump in the second and third rounds. This modification was found to be critical to the formation of Au nanospheres with diameters larger than 30 nm due to the large length scale involved in the diffusion of surface atoms. To confirm the role played by the injection rate of Au precursor in determining the formation of Au nanospheres, we varied the injection rate of precursor solution in the second round. As shown in **Figure 5**, for the 23-nm Au nanospheres, if the precursor solution was injected in one-shot while all other parameters were kept the same; the products were dominated by cubic Au nanocrystals (**Figure 5a**). A slightly slower injection rate would still lead to the formation of nanocrystals with nonspherical shapes. Specifically, when the

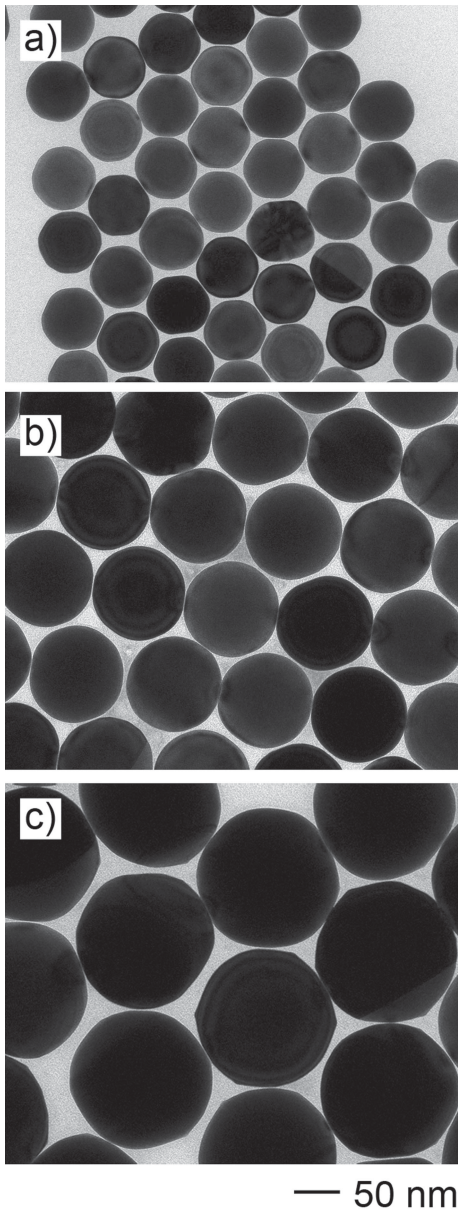


**Figure 4.** TEM images of single-crystal Au nanospheres with controlled diameters in the range of 70–150 nm: a) 70 nm; b) 100 nm; and c) 150 nm. They were obtained using the standard dropwise injection procedure, except that the volumes of the 46-nm seed solution were: a) 1500  $\mu$ L; b) 500  $\mu$ L; and c) 50  $\mu$ L, respectively.

injection rates were set to 1  $\text{mL h}^{-1}$  and 0.5  $\text{mL h}^{-1}$ , cuboctahedrons and truncated octahedrons (Figure 5b,c) were obtained, respectively. These results indicate the critical role played by the injection rate of Au precursor in maintaining the spherical shape during seed-mediated growth.

As demonstrated in our recent study, the growth pattern of a seed is governed by the ratio between the rates for atom deposition and surface diffusion.<sup>[65]</sup> Considering that the rate for surface diffusion is mainly determined by the reaction temperature and each set of the experiments were conducted under the same conditions except for the injection rate of Au

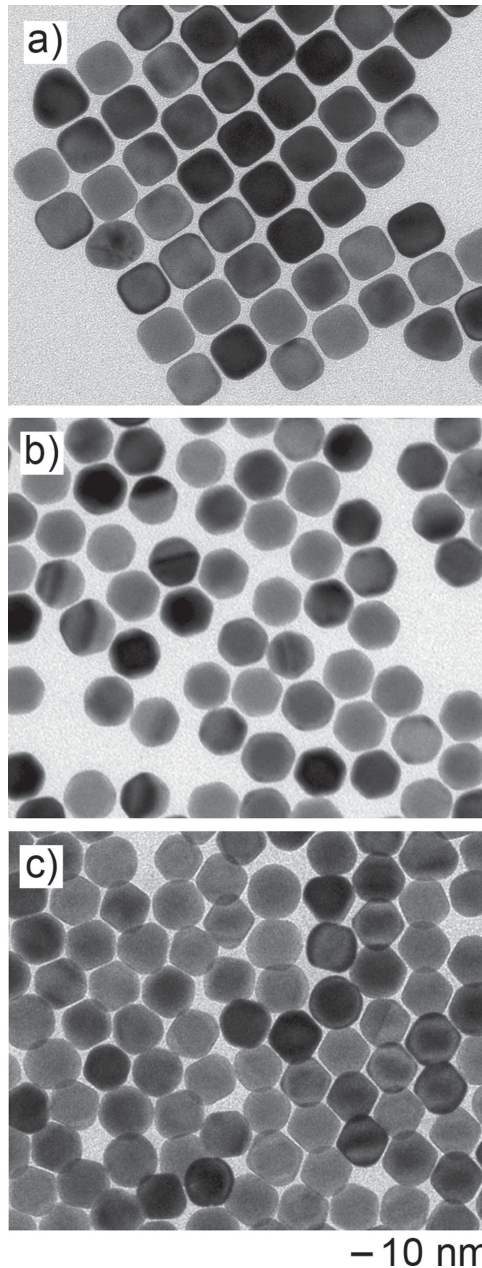


**Figure 5.** The effect of injection rate of Au precursor on the morphology of final products. TEM images of Au nanocrystals that were prepared using the same procedure as the 23-nm Au nanospheres, except that 2 mL of Au precursor solution was added via a) one-shot injection and b,c) dropwise introduction at injection rates of b) 1  $\text{mL h}^{-1}$  and c) 0.5  $\text{mL h}^{-1}$ , respectively.

precursor, the diffusion rate was supposed to be fixed and thus the observed shape variations could be attributed to the change in deposition rate. When the Au precursor was rapidly injected into a reaction solution, the growth should be dominated by atom deposition only as surface diffusion over a large length scale could be neglected. A preferential deposition along <111> directions on a spherical seed led to the formation of nanocube mainly covered by {100} facets.<sup>[66]</sup> In contrast, when Au precursor solution was added slowly in a dropwise manner, the

deposition rate would be significantly reduced. In this case, the newly deposited Au atoms could have sufficient time to migrate to adjacent {100} facets. As a result, the growth pathway, enabled by surface diffusion, became partially switched to <100> directions, leading to a gradually reduced proportion for {100} facets in the final product and truncated octahedrons would be formed. At a moderate injection rate for Au precursor, the growth rates along the <111> and <100> directions could become roughly the same, making it possible to maintain the shape spherical Au seeds during successive, seed-mediated growth.

### 3.3. The Effect of the Reductant Concentration

We also investigated the role of reductant (AA) concentration in the formation of Au nanospheres. Figure 6 shows the products obtained using the same procedure except for the variation of AA amount. When the amount of AA was increased from 1.3  $\mu\text{mol}$  to 1.5  $\mu\text{mol}$ , the products were still dominated by nanocrystals with a spherical profile (Figure 6a). At relatively larger amounts of AA (e.g., 2.0  $\mu\text{mol}$  and 3.0  $\mu\text{mol}$ ), we observed a noticeable loss of spherical shape for the resultant Au nanocrystals (Figure 6b,c). Although a limited supply of Au precursor was involved due to the dropwise addition of HAuCl<sub>4</sub>, a relatively high concentration of AA could still accelerate the reduction and thus increase the deposition rate.<sup>[25,27,67]</sup> Taken together, an appropriate ratio between the rates for atom deposition and surface diffusion was critical to promoting the growth of seeds into larger particles without losing the spherical shape. In general, fast deposition rates or slow surface diffusion rates would force the spherical seeds to evolve into nonspherical ones.

### 3.4. The Effect of Halide Ions (Br<sup>-</sup> and I<sup>-</sup>)

Besides the injection rate for the Au precursor and the amount of reductant, we also tried to modulate the reaction by varying the type of halide ions present in the system. When Br<sup>-</sup> anions were added into the reaction system, the products were dominated by nanocrystals with a cubooctahedral shape (Figure 7a). A replacement of Br<sup>-</sup> ions by I<sup>-</sup> ions at the same concentration would lead to the formation of Au nanocrystals exhibiting a truncated octahedral profile (Figure 7b). In both cases, the presence of Br<sup>-</sup> or I<sup>-</sup> ions, in addition to Cl<sup>-</sup> anions, could no longer promote the formation of Au nanocrystals with a spherical profile. This shape variation may arise from the difference in affinity between halide ions toward the surface of Au nanocrystals. According to hard and soft Lewis acids and bases (HSAB) theory, a larger and less electronegative halide can have an increasing binding affinity with Au.<sup>[68]</sup> Therefore, a higher affinity to the surface of Au nanocrystals should be expected when either Br<sup>-</sup> or I<sup>-</sup> anions were present.<sup>[69-73]</sup> Their interactions may have changed the growth mode and thus be responsible for the observed shape variation. Unlike the common use of CTAB in the previous syntheses of Au nanocrystals, i.e., rods and octahedrons, we include sufficient amount of CTAC in the current synthesis. The use of CTAC not only protected

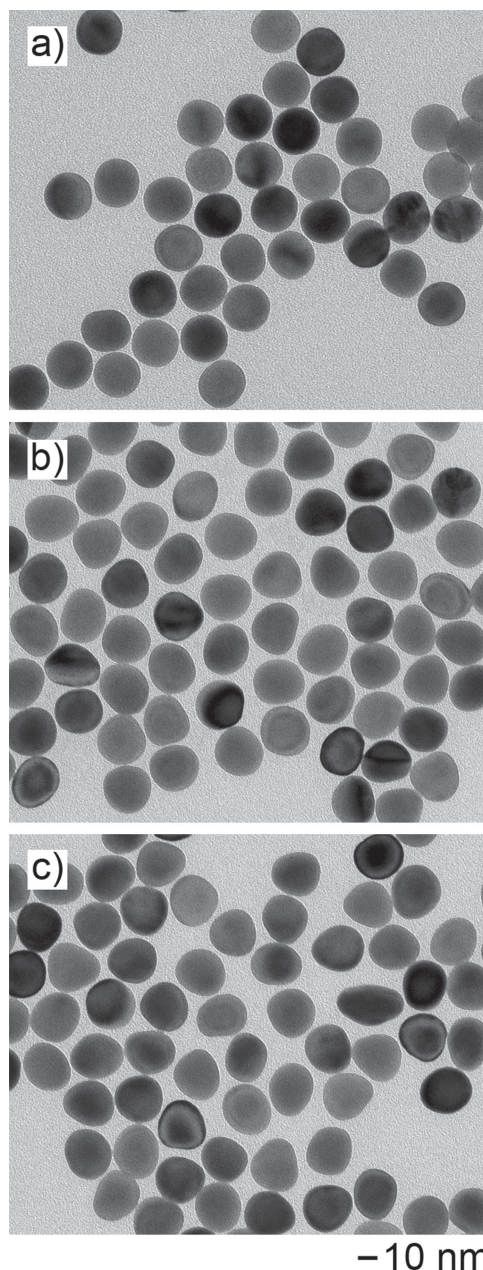


**Figure 6.** The effect of the amount of reductant (AA) on the morphology of final products. TEM images of Au nanocrystals that were prepared using the same procedure as the 23-nm Au nanospheres, except that the amount of AA was increased from 1.3  $\mu\text{mol}$  to a) 1.5  $\mu\text{mol}$ ; b) 2.0  $\mu\text{mol}$ ; and c) 3.0  $\mu\text{mol}$ , respectively.

nanocrystals from aggregations, but also completely excluded those halide anions with larger affinity with Au from the reaction system and thus contributed to the growth of spherical seeds without noticeable shape change.<sup>[74,75]</sup>

## 4. Conclusions

In summary, we have successfully synthesized single-crystal Au nanospheres with controlled diameters in the range of

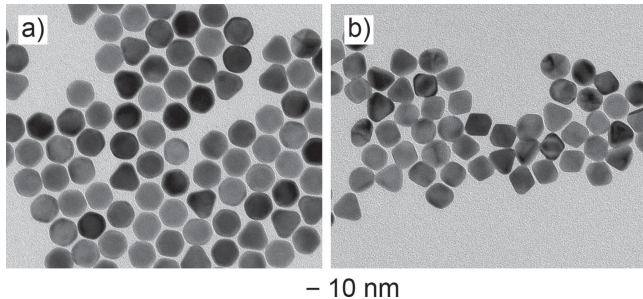


**Figure 7.** The effect of halide ions on the morphology of final products. TEM images of Au nanocrystals that were prepared using the same procedure as the 23-nm Au nanospheres, except for the additional 10  $\mu\text{mol}$  of a) KBr and b) KI, respectively.

5–150 nm via successive seed-mediated growth. In the first step, we obtained Au nanospheres with diameters tunable in the range of 5–16 nm by varying the amount of CTAB-capped Au clusters that served as the initial seeds. In the second round, the as-obtained 10-nm Au nanospheres served as the seeds to generate Au nanospheres with diameters continuously tunable from 15 to 80 nm. Following the same protocol for the second round, the next step involved the use of the 46-nm Au nanospheres as the seeds to synthesize Au nanospheres with even larger diameters in the range of 70–150 nm. We found that the dropwise injection of Au precursor solution using a syringe pump, a relatively low amount of reductant, and the absence of halide anions with strong affinity toward Au in the second and third rounds were all critical to the formation of spherical Au nanocrystals in high yields. This work offers a simple and robust route to the synthesis of single-crystal Au nanospheres with uniform, controllable diameters over a broad range from 5 to 150 nm, which will find immediate use in the syntheses of bimetallic nanostructures, fabrication of metallic photonic crystals, and biomedical research.

## Supporting Information

Supporting Information is available from the Wiley Online Library or from the author.

## Acknowledgement

This work was supported in part by the NSF (DMR-1215034) and startup funds from Georgia Institute of Technology. The authors thank Yin Yang and Dr. Dong Qin for their help with the use of their DLS instrument.

Received: July 15, 2013

Published online: August 26, 2013

- [5] C. J. Murphy, A. M. Gole, J. W. Stone, P. N. Sisco, A. M. Alkilany, E. C. Goldsmith, S. C. Baxter, *Acc. Chem. Res.* **2008**, *41*, 1721.
- [6] A. A. Herzing, C. J. Kiely, A. F. Carley, P. Landon, G. J. Hutchings, *Science* **2008**, *321*, 1331.
- [7] S. Eustis, M. A. El-Sayed, *Chem. Soc. Rev.* **2006**, *35*, 209.
- [8] C. D. Pina, E. Faletta, M. Rossi, *Chem. Soc. Rev.* **2012**, *41*, 350.
- [9] E. C. Dreaden, A. M. Alkilany, X. Huang, C. J. Murphy, M. A. El-Sayed, *Chem. Soc. Rev.* **2012**, *41*, 2740.
- [10] H. Chen, L. Shao, Q. Li, J. Wang, *Chem. Soc. Rev.* **2013**, *42*, 2679.
- [11] T. L. Doane, C. Burda, *Chem. Soc. Rev.* **2012**, *41*, 2885.
- [12] C. J. Orendorff, T. K. Sau, C. J. Murphy, *Small* **2006**, *2*, 636.
- [13] C. L. Nehl, J. H. Hafner, *J. Mater. Chem.* **2008**, *18*, 2415.
- [14] J. N. Anker, W. P. Hall, O. Lyandres, N. C. Shah, J. Zhao, R. P. Van Duyne, *Nat. Mater.* **2008**, *7*, 442.
- [15] C. E. Talley, J. B. Jackson, C. Oubre, N. K. Grady, C. W. Hollars, S. M. Lane, T. R. Huser, P. Nordlander, N. J. Halas, *Nano Lett.* **2005**, *5*, 1569.
- [16] P. C. Ray, *Chem. Rev.* **2010**, *110*, 5332.
- [17] S. Link, M. A. El-Sayed, *Int. Rev. Phys. Chem.* **2000**, *19*, 409.
- [18] S. Link, M. A. El-Sayed, *J. Phys. Chem. B* **1999**, *103*, 8410.
- [19] Y. Zheng, J. Tao, H. Liu, J. Zeng, T. Yu, Y. Ma, C. Moran, L. Wu, Y. Zhu, J. Liu, Y. Xia, *Small* **2011**, *7*, 2307.
- [20] K. Zhou, Y. Li, *Angew. Chem. Int. Ed.* **2012**, *51*, 602.
- [21] L. M. Molina, B. Hammer, *Appl. Catal. A* **2005**, *291*, 21.
- [22] T. K. Sau, C. J. Murphy, *J. Am. Chem. Soc.* **2004**, *126*, 8648.
- [23] F. Kim, S. Connor, H. Song, T. Kuykendall, P. Yang, *Angew. Chem. Int. Ed.* **2004**, *43*, 3673.
- [24] D. Seo, J. C. Park, H. Song, *J. Am. Chem. Soc.* **2006**, *128*, 14863.
- [25] W. Niu, S. Zheng, D. Wang, X. Liu, H. Li, S. Han, J. Chen, Z. Tang, G. Xu, *J. Am. Chem. Soc.* **2008**, *131*, 697.
- [26] B. Nikoobakht, M. A. El-Sayed, *Chem. Mater.* **2003**, *15*, 1957.
- [27] H.-L. Wu, C.-H. Kuo, M. H. Huang, *Langmuir* **2010**, *26*, 12307.
- [28] N. R. Jana, L. Gearheart, C. J. Murphy, *J. Phys. Chem. B* **2001**, *105*, 4065.
- [29] D. Seo, C. I. Yoo, I. S. Chung, S. M. Park, S. Ryu, H. Song, *J. Phys. Chem. C* **2008**, *112*, 2469.
- [30] A. Sánchez-Iglesias, I. Pastoriza-Santos, J. Pérez-Juste, B. Rodríguez-González, F. J. García de Abajo, L. M. Liz-Marzán, *Adv. Mater.* **2006**, *18*, 2529.
- [31] J. E. Millstone, S. Park, K. L. Shuford, L. Qin, G. C. Schatz, C. A. Mirkin, *J. Am. Chem. Soc.* **2005**, *127*, 5312.
- [32] J. Zhang, M. R. Langille, M. L. Personick, K. Zhang, S. Li, C. A. Mirkin, *J. Am. Chem. Soc.* **2010**, *132*, 14012.
- [33] Y. Ma, Q. Kuang, Z. Jiang, Z. Xie, R. Huang, L. Zheng, *Angew. Chem. Int. Ed.* **2008**, *47*, 8901.
- [34] T. Ming, W. Feng, Q. Tang, F. Wang, L. Sun, J. Wang, C. Yan, *J. Am. Chem. Soc.* **2009**, *131*, 16350.
- [35] T. T. Tran, X. Lu, *J. Phys. Chem. C* **2011**, *115*, 3638.
- [36] B. J. Wiley, S. H. Im, Z.-Y. Li, J. McLellan, A. Siekkinen, Y. Xia, *J. Phys. Chem. B* **2006**, *110*, 15666.
- [37] Y. Wang, M. Ibisate, Z. Y. Li, Y. Xia, *Adv. Mater.* **2006**, *18*, 471.
- [38] B. D. Chithrani, A. A. Ghazani, W. C. W. Chan, *Nano Lett.* **2006**, *6*, 662.
- [39] B. D. Chithrani, W. C. W. Chan, *Nano Lett.* **2007**, *7*, 1542.
- [40] P. Ghosh, G. Han, M. De, C. K. Kim, V. M. Rotello, *Adv. Drug Delivery Rev.* **2008**, *60*, 1307.
- [41] N. Khlebtsov, L. Dykman, *Chem. Soc. Rev.* **2011**, *40*, 1647.
- [42] X.-D. Zhang, D. Wu, X. Shen, P.-X. Liu, N. Yang, B. Zhao, H. Zhang, Y.-M. Sun, L.-A. Zhang, F.-Y. Fan, *Int. J. Nanomedicine* **2011**, *6*, 2071.
- [43] M. Eguchi, D. Mitsui, H.-L. Wu, R. Sato, T. Teranishi, *Langmuir* **2012**, *28*, 9021.
- [44] Y. Zheng, Y. Ma, J. Zeng, X. Zhong, M. Jin, Z.-Y. Li, Y. Xia, *Chem. Asian J.* **2013**, *8*, 792.
- [45] J. Li, Y. Zheng, J. Zeng, Y. Xia, *Chem. Eur. J.* **2012**, *18*, 8150.

- [1] M.-C. Daniel, D. Astruc, *Chem. Rev.* **2003**, *103*, 293.
- [2] K. Saha, S. S. Agasti, C. Kim, X. Li, V. M. Rotello, *Chem. Rev.* **2012**, *112*, 2739.
- [3] A. M. Alkilany, S. E. Lohse, C. J. Murphy, *Acc. Chem. Res.* **2012**, *46*, 650.
- [4] D. A. Giljohann, D. S. Seferos, W. L. Daniel, M. D. Massich, P. C. Patel, C. A. Mirkin, *Angew. Chem. Int. Ed.* **2010**, *49*, 3280.

- [46] Y. Ma, W. Li, E. C. Cho, Z. Li, T. Yu, J. Zeng, Z. Xie, Y. Xia, *ACS Nano* **2010**, *4*, 6725.
- [47] J. Zeng, Y. Zheng, M. Rycenga, J. Tao, Z.-Y. Li, Q. Zhang, Y. Zhu, Y. Xia, *J. Am. Chem. Soc.* **2010**, *132*, 8552.
- [48] J. Rodríguez-Fernández, J. Pérez-Juste, F. J. García de Abajo, L. M. Liz-Marzán, *Langmuir* **2006**, *22*, 7007.
- [49] H. Hiramatsu, F. E. Osterloh, *Chem. Mater.* **2004**, *16*, 2509.
- [50] C. Gao, J. Vuong, Q. Zhang, Y. Liu, Y. Yin, *Nanoscale* **2012**, *4*, 2875.
- [51] Z. Wang, B. Tan, I. Hussain, N. Schaeffer, M. F. Wyatt, M. Brust, A. I. Cooper, *Langmuir* **2006**, *23*, 885.
- [52] N. R. Jana, L. Gearheart, C. J. Murphy, *Langmuir* **2001**, *17*, 6782.
- [53] J.-P. Deng, C. Wu, C.-H. Yang, C.-Y. Mou, *Langmuir* **2005**, *21*, 8947.
- [54] N. R. Jana, X. Peng, *J. Am. Chem. Soc.* **2003**, *125*, 14280.
- [55] D. A. Fleming, M. E. Williams, *Langmuir* **2004**, *20*, 3021.
- [56] I. Hussain, S. Graham, Z. Wang, B. Tan, D. C. Sherrington, S. P. Rannard, A. I. Cooper, M. Brust, *J. Am. Chem. Soc.* **2005**, *127*, 16398.
- [57] X. Ji, X. Song, J. Li, Y. Bai, W. Yang, X. Peng, *J. Am. Chem. Soc.* **2007**, *129*, 13939.
- [58] N. G. Bastús, J. Comenge, V. Puntes, *Langmuir* **2011**, *27*, 11098.
- [59] X. Liu, H. Xu, H. Xia, D. Wang, *Langmuir* **2012**, *28*, 13720.
- [60] N. Pazos-Perez, F. J. Garcia de Abajo, A. Fery, R. A. Alvarez-Puebla, *Langmuir* **2012**, *28*, 8909.
- [61] R. Pecora, *Dynamic Light Scattering: Applications of Photon Correlation Spectroscopy*, Plenum, New York **1985**.
- [62] B. N. Khlebtsov, N. G. Khlebtsov, *Colloid J.* **2011**, *73*, 118.
- [63] V. V. Klyubin, L. A. Kruglova, H. A. Sakharova, Y. A. Tallier, *Kolloidn. Zh.* **1990**, *52*, 470.
- [64] V. V. Klyubin, V. N. Bungov, *Kolloidn. Zh.* **1998**, *60*, 344.
- [65] X. Xia, S. Xie, M. Liu, H.-C. Peng, N. Lu, J. Wang, M. J. Kim, Y. Xia, *Proc. Natl. Acad. Sci. USA* **2013**, *110*, 6669.
- [66] Z. L. Wang, *J. Phys. Chem. B* **2000**, *104*, 1153.
- [67] M. R. Langille, M. L. Personick, J. Zhang, C. A. Mirkin, *J. Am. Chem. Soc.* **2012**, *134*, 14542.
- [68] R. G. Pearson, *J. Am. Chem. Soc.* **1963**, *85*, 3533.
- [69] P.-J. Chung, L.-M. Lyu, M. H. Huang, *Chem. Eur. J.* **2011**, *17*, 9746.
- [70] J. E. Millstone, W. Wei, M. R. Jones, H. Yoo, C. A. Mirkin, *Nano Lett.* **2008**, *8*, 2526.
- [71] D. K. Smith, N. R. Miller, B. A. Korgel, *Langmuir* **2009**, *25*, 9518.
- [72] R. G. Rayavarapu, C. Ungureanu, P. Krystek, T. G. van Leeuwen, S. Manohar, *Langmuir* **2010**, *26*, 5050.
- [73] C. J. Murphy, L. B. Thompson, D. J. Chernak, J. A. Yang, S. T. Sivapalan, S. P. Boulos, J. Huang, A. M. Alkilany, P. N. Sisco, *Curr. Opin. Colloid Interface Sci.* **2011**, *16*, 128.
- [74] M. Tréguer-Delapierre, J. Majimel, S. Mornet, E. Duguet, S. Ravaine, *Gold Bull.* **2008**, *41*, 195.
- [75] C. J. Murphy, T. K. Sau, A. M. Gole, C. J. Orendorff, J. Gao, L. Gou, S. E. Hunyadi, T. Li, *J. Phys. Chem. B* **2005**, *109*, 13857.